Contribution of settling measurements to the study of polycyclic aromatic hydrocarbons' (PAHs) mobilisation during resuspension of PAHs-associated sediment

Gisèle Usanase, Nathalie Azéma, Youssef El Bitouri, Jean-Claude Souche, Catherine Gonzalez

Contribution of settling measurements to the study of polycyclic aromatic hydrocarbons' (PAHs) mobilisation during resuspension of PAHs-associated sediment

Gisèle Usanase[1] · Nathalie Azema[1] · Youssef El Bitouri[1] · Jean-Claude Souche[1] · Catherine Gonzalez[2]

Abstract
This paper aims to investigate the effect of the settling behaviour of sediment particles during resuspension on the mobilisation of pollutants such as polycyclic aromatic hydrocarbons (PAHs). Sediments were collected in different areas (basin, channel, beach) of a Mediterranean harbour, located in the south of France (the Grau du Roi harbour), and then separated into different size fractions: large (80–1000 pm), intermediate (40–80 pm), and fine (< 40 pm). Total PAHs concentrations in the initial sediment ranged from 320 to 1043 pg kg^{-1}. Study of the settling behaviour of the PAH-contaminated sediment revealed two sedimentation regimes: sedimentation by mass, which exhibits a sharp interface between the supernatant and the deposit, and sedimentation by clarification with no interface. ft appears that sediment particles settle either by the clarification regime or by a combination of the two sedimentation regimes, depending on the size fraction. Particle size distribution monitoring during the settling process allowed the identification of sediment particles less than 20 pm which remain in the water column up to 20 min after resuspension and appear to be the ones that can potentially mobilise PAHs.

Keywords Polycyclic aromatic hydrocarbons (PAHs) · Marine sediment · Resuspension · Settling · Particle size distribution (PSD)

Introduction

In the aquatic environment, sediment resuspension may occur as a result of natural distuibance events (hurricanes storms, strong physical currents, etc.) or through human activity (dredging) (Bourrin et al. 2008; Capello et al. 2016; Coulon 2014; Ferré et al. 2005; Spearman 2015) . However, sediments constitute an important source of inorganic and organic contaminants for the marine environment (Huntingford and Turner 2011). A large variety of contaminants, including polycyclic aromatic hydrocarbons (PAHs), polychlorobiphenyls (PCB), dioxin, pesticides, heavy metals, and other pollutants from industrial, agricultural, urban, and maritime activities are associated with sediment particles (Ahrens and Depree 2004; Baumard et al. 1998; Belles et al. 2017; Cutroneo et al. 2015; Ghosh et al. 2003). Sediment contamination is of great environmental concern due to its potentially toxic effects on biological and ecological resources as well as on human health. Currently, environmental managers are tasked with making decisions involving the fate of contaminated sediment. Information on the fate of resuspended sediment is required in order to be able to make decision about the monitoring and management of these sediments in the case of resuspension.

Bottom sediment disturbance can cause resuspension of contaminated sediments in the water column. These resuspended particles pose significant water quality concerns as they may affect the transport of associated contaminants. Once in the water column, different processes can act on suspended sediment particles and may render mobile pollutants that were previously bound (Cantwell and Burgess 2004). Concerns about the mobilisation of contaminants usually include biological and ecological impacts in the immediate vicinity of resuspension event and the potential for contaminants to spread into previously unaffected areas (Je et al. 2007).

El Youssef El Bitouri
youssef.elbitouri@mines-ales.fr

[i] LMGC, IMT Mines Alès, Univ Montpellier, CNRS, Ales, France

[2] LGE1, IMT Mines Alès, Alès, France

This study focuses on PAHs, which are ubiquitous contaminants in the environment and are generated by natural and anthropogenic processes. These compounds can be introduced into the environment in various ways and are usually composed of two or more of these compounds (Abdel-Shafy and Mansour 2016). PAHs are of environmental concern due to their toxic, mutagenic, and carcinogenic potential (IARC 1983). Given their physical and chemical properties, PAHs seem to be a relevant choice for this study as they have a low solubility and are preferentially bonded to sediment particles (Latimer et al. 1999). The present study focuses on the 16 PAHs designated as priority pollutants by the United States Environmental Protection Agency (US EPA) (United States Environmental Protection Agency (USEPA) 1993).

The mobilisation of PAHs during sediment resuspension events can result from various and complex processes: granular behaviour of sediments (resuspension, agglomeration/dispersion) or physicochemical process (release of PAHs by adsorption/desorption and PAH dissolution/precipitation) (Dong et al. 2016; Feng et al. 2008; Latimer et al. 1999; Vagge et al. 2018). Previous studies have shown that the distribution of PAHs varies depending on the different size and density fractions of contaminated sediments (Ahrens and Depree 2004; Simpson et al. 1996). Fine sediments are expected to be resuspended more easily during dredging operations (Feng et al. 2008; Guigue et al. 2018; Hayes 1986). Depending on the research field, the concept of "fine sediment" varies, but in general, particles less than 63 μm are defined as fine sediments (Ahrens and Depree 2004; Capello et al. 2016; Ferré et al. 2005; Guigue et al. 2018; Hayes 1986). These fine sediments have low settling velocities and can remain in suspension for extended periods. Consequently, they may be transported significant distances away from the initial action, up to 3 km from in case of dredging operations (Spearman 2015). Also, the more contaminated sediment remains suspended in the water column, the more they are likely to release sediment-associated PAHs and/or freely dissolved PAHs (by desorption) into the water (Dong et al. 2016; Feng et al. 2008). Therefore, a better understanding of PAH distribution in size fractions of sediment allows processes that may occur during resuspension to be elucidated. The fate of particles during transportation can be inferred from their settling velocity. The settling velocity depends on a range of variables, including particle size, density and shape of the sediment, volume fraction of suspension, viscosity and nature of the suspending medium (Bru et al. 2004; Chhabra 2019; Wendling et al. 2015). However, particle size appears to be a determining parameter (Chhabra 2019). Settling velocity of suspended particles is a dominant factor controlling the transfer and fate of sediment and sediment-associated substances such as contaminants. Contaminant transportation is largely determined by the dynamics of the system and contaminant-particle association (Latimer et al. 1999).

The aim of this study is to explore different factors which might have an influence on the settling behaviour of sediment particles resuspended in the water column and consequently on associated substances such as contaminating PAHs. For this purpose, a dual experimental approach combining sediment contamination characterisation (PAHs concentration and origin determination) and sediment settling behaviour was used. Sediments were collected from the Grau du Roi harbour located in the city of Grau du Roi in the Gulf of Lion (Mediterranean Sea) in the south of France, and then separated into different size fractions. Parameters which could affect PAHs distribution in sediments such as particle size, surface area, and organic matter content were also investigated. After induced resuspension, settling behaviour of size fractions of the PAHs-contaminated sediment is studied in a laboratory setting, in order to better understand the sedimentation process after a resuspension event. Parameters that can affect the settling behaviour such as particle size distribution and volume fraction were additionally examined. During the sedimentation process, an optical measurement technique (Turbiscan Lab) was used to capture both temporal and spatial changes in the studied suspension and was complimented by size distribution monitoring within the column. Moreover, the use of Turbiscan Lab presents operational advantages such as easy modification of testing protocols, application of controlled conditions (known levels of resuspension energy, use of artificial seawater). and also the study of a small sample size. Knowledge of PAHs contamination levels and distribution in the size fractions as well as the settling behaviour of those size fractions makes it possible to identify and better understand parameters governing PAHs mobilisation during resuspension events.

Materials and methods

Sampling site and sediment

The sampling site is the Grau du Roi harbour located in the city of Grau du Roi in the south of France. It is the second most important fishing port in the French Mediterranean and has the capacity to harbour up to 200 boats. Surrounding the harbour area is a nature reserve (Natura 2000) classified as protected by the European Union in order to maintain the exceptional biodiversity of the site. Additionally, nearby is Port Camargue, one of the biggest marinas in Europe, as well as many areas for bathing. The presence of these important sites near the Grau du Roi harbour highlights the necessity to study and control the mobilisation of pollutants.

Sediment was collected by divers using a hand-held Van Veen grabber at depth ranges between 2 and 4 m in several zones aiming to study a set of different and representative characteristics (size distribution, chemical composition) of

sediments from the Grau du Roi harbour. Samples were collected from the fishing basin (B), the navigation channel (C) and in the sea in front of the beach (Sb) which can be seen in Fig. 1. Following sampling, all the sediment samples were put in glass jars and stored at 4 °C in the dark.

Artificial seawater preparation

Artificial seawater (ASW) of 35.0 salinity was prepared by mixing six of the major components that constitute seawater (Brzozowska et al.. 2012). Specifically, it consists of NaCl (24.5 g kg^{-1}), $MgCl_2$ (5.2 g kg^{-1}), Na_2SO_4 (4.1 g kg^{-1}), $CaCl_2$ (1.2 g kg^{-1}), KCl (0.7 g kg^{-1}), and $NaHCO_3$ (0.2 g kg^{-1}). Dilutions of ASW were prepared with ultrapure water (18 MΩ cm, Millipore Synergy UV system). The ASW was used in the preparation of all studied suspensions, in order to work in controlled media but remaining close to the marine conditions. The prepared seawater had a pH of 7.1 ± 0.2 and conductivity of 51 ± 1 mS.

Wet sieving and pore water extraction

Wet sieving was performed using artificial sea water (ASW) so as to not denature the samples by remaining in conditions as representative as possible of the natural environment. For each sediment sample, the bulk fraction was sieved with a 1-mm mesh in order to remove all visible debris such as vegetation, shells, and wood.

Size fractions (80–1000 μm, 40–80 μm, and < 40 μm) were obtained by wet sieving sediment suspensions through 1000-μm, 80-μm, and 40-μm meshes according to the Renard series NF ISO 3310-1, X11-514-1 (2019). Only three fractions were obtained due to technical difficulties and the available quantity of sediment samples. The 80–1000 μm, 40–80 μm, and < 40 μm fractions will be referred to, respectively, as the large fraction, the intermediate fraction, and the fine fraction. After the sieving process, pore water was extracted by centrifugation at 1000 rpm during 15 min from the bulk sediment (< 1 mm) and from all the different size fractions.

Granular and physical characterisation of sediments

Particle size distributions (PSD) of studied sediments in artificial seawater were obtained using a laser granulometer LS 13320 from the Beckman Coulter company. An optical model was defined with a refractive index including a real part of 1.57 and an imaginary part of 0.3.

An environmental scanning electron microscope with energy-dispersive X-ray spectroscopy (SEM–EDX) (Quanta 200 FEG) from the FEI was used.

Freeze-dried sediment surface areas were measured by nitrogen adsorption (BET method) using a SA3100 surface area analyser from Beckman Coulter. Brunauer–Emmett–Teller method was used to determine sediment surface area (S_{BET}).

Density was measured using the AccuPyc 1330 pycnometer from Micromeritics. Water content (% water) was

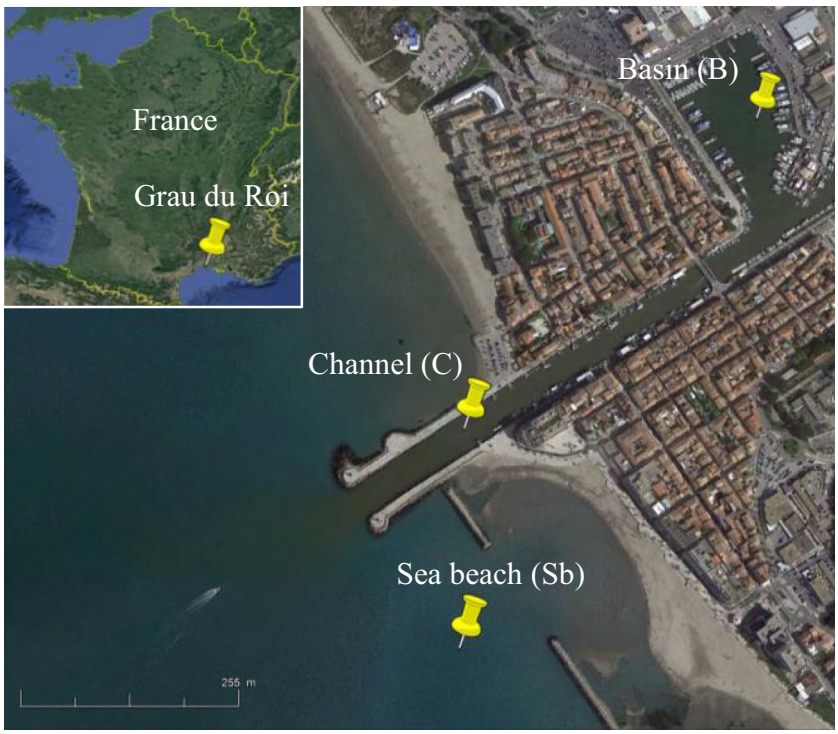

Fig. 1 Sampling sites, different areas where sediment samples were collected from the Grau du Roi harbour

determined by difference in mass weighed before and after drying at 105 °C for 96 h.

Chemical and crystallographic characterisation

The SEM–EDX mentioned above was also used to quantify elemental chemical composition of the sediment.

After drying (40 °C for 72 h) and grinding, crystallographic analyses of the sediment were performed by X-ray diffractometry (XRD) using a Brüker AXS diffractometer with CuKα radiation (λ = 1.54178 Å) to determine their mineral composition.

Total organic carbon (TOC) measurements were performed on bulk sediment and fractions after freeze-drying using a VarioTOC CUBE from ELEMENTAR. The device vaporises the solution at 850 °C and measures the total quantity of carbon released with an infrared detector (detection of CO_2 band).

PAH concentrations were determined for the 16 PAHs studied: naphthalene (Na), acenaphthylene (Acy), acenaphthene (Ace), fluorene (Flu), phenanthrene (Phe), anthracene (Ant), fluoranthene (Fla), pyrene (Py), benzo(a)anthracene (BaA), chrysene (Chr), benzo(b)fluoranthene (BbF), benzo(k)fluoranthene (BkF), benzo(a)pyrene (BaP), indeno (1,2,3-c,d)pyrene (IP), dibenz(ah)anthracene (DahA), and benzo(ghi)perylene (BghiP). PAHs analysis was adapted from the analytical protocol described by Barhoumi et al. (Barhoumi et al. 2014) and Bancon-Montigny et al. (Bancon-Montigny et al. 2019). PAHs were extracted from the sample using the accelerated solvent extraction (ASE) technique (ASE 350 Dionex). The extracted PAHs were then analysed using gas chromatography coupled with mass spectrometry (GC–MS). An amount of freeze-dried sediment (3 to 5 g) was introduced into the stainless steel extraction cell in order to extract the PAHs. Recovery standards for the PAHs (naphthalene d8, acenaphthene d10, acenaphthylene d8, phenanthrene d10, fluoranthene d10) were also added in the cell before extraction. ASE extraction was carried out for 15 min with a solvent mixture (hexane/acetone (50/50)) at 120 °C and 1500 psi of nitrogen. The extract was then kept in contact with copper powder for 48 hours in order to remove any sulphur. Following this, the extract was purified by solid-phase extraction (SPE) using Strata Florisil cartridges (FL-PR, 32138). Purified extracts were analysed by GC–MS (Varian 450-GC and Varian 240 MS) working with the electron impact mode at 70 eV. A DB-5ms (Agilent) chromatographic column (30 m, 0.25 mm ID, and 0.25 μm of film thickness) was used. Helium flow rate was fixed at 1 mL min^{-1}. The extract (2 μL) was injected onto the chromatographic column with a PTV 1079 injector maintained at 300 °C. Initial temperature of the oven was programmed to 80 °C (holding for 2 min), then increased at a rate of 10 °C.min^{-1} to 200 °C (holding for 5 min), and increased again to 240 °C at a rate of 5 °C/min (holding for 5 min). Finally, the temperature was raised to 300 °C at a 6 °C min^{-1} rate and held for 8 min. Identification and quantification of the 16 PAHs in the samples were achieved by matching the compound ion and retention time with those of a standard mixture of PAHs. The PAHs analysis process (extraction, clean up, and GC/MS analysis) was validated using a certified sediment CNS391-50G (Sigma Aldrich).

Settling behaviour measurement

The settling behaviour was studied using Turbiscan Lab from Formulaction. The evolution of particle size distribution during settling was also monitored using a laser granulometer. Simultaneously to the monitoring of settling behaviour, particle size distribution of sediment remaining in the supernatant was also followed over time. Both studies offer complementary information in order to understand sediment settling behaviour and to identify which size fraction could remain in suspension in the water column. The procedure used is illustrated in Fig. 2.

In a beaker, suspensions with a given volume fraction (Φ_V) were prepared by mixing sediment with artificial seawater (ASW) for 20 min using a magnetic stirrer. For each suspension, a volume of 20 mL was put in the analysis cell (27.5-mm diameter and 72.5-mm height) and sediment settling (first sedimentation) was analysed by the Turbiscan Lab® at room temperature (25 °C). In order to mimic dredging conditions, resuspension was induced by mechanical stirring (500 rpm) directly in the analysis cell for 5 min using a paddle as shown in Fig. 2. This second settling process will be referred to as "resedimentation".

The Turbiscan Lab principle of measurement is based on the irradiation of a sample with a near-infrared light of 808 nm and detection of the transmitted (T) and backscattered (BS) signal as a function of time and cell height. According to turbidity of the suspension, the emitted light is either transmitted or backscattered. These two signals each measure 40 μm and based on the following equations (Bru et al. 2004):

$$\%\boldsymbol{BS} \approx \sqrt{\frac{dh}{\lambda^*}} \qquad \%\boldsymbol{T} = \exp\left(\frac{-2r}{\lambda}\right)$$
$$\text{With}\lambda^* = \frac{2d}{3\Phi(1-g)Q_s} \quad \text{and} \quad \lambda = \frac{\lambda^*}{1-g} \tag{1}$$

where $\boldsymbol{\lambda}$ is the wavelength (mean free path), $\boldsymbol{\lambda^*}$ is the transport mean free path, $\boldsymbol{dh}$ is the thickness of the backscattered signal detector, d is the average particle diameter, $\boldsymbol{r}$ is the average particle radius, $\boldsymbol{\Phi}$ is the volume fraction occupied by particles, $\boldsymbol{g}$ is the asymmetry factor, and $\boldsymbol{Qs}$ is the diffusion efficiency.

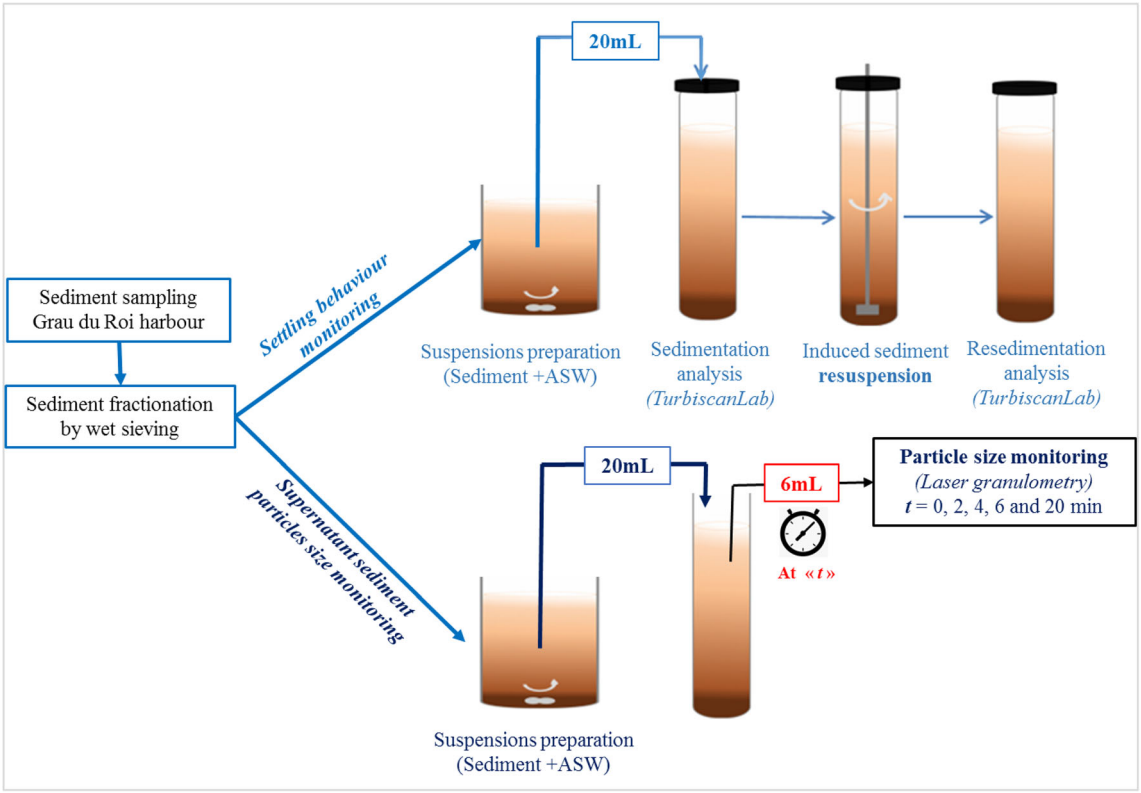

Fig. 2 Schema of the operating procedure used for sediment resuspension in order to monitor their settling behaviour after an induced resuspension

BS and T profiles resulting from the Turbiscan lab analysis provide information about destabilisation processes, such as particle migration (sedimentation in this case) or particle size evolution (agglomeration for example). BS and T profiles and parameters used to characterise settling will be developed in the "Sediment settling behaviour" section.

For each studied sediment, five suspensions were prepared and used to monitor sediment particle size during the settling behaviour study: 6 mL of the suspension were collected at five different times of settling (0, 2, 4, 6, and 20 min) and particle size distribution in the supernatant was determined by laser granulometry (Fig. 2).

Results and discussion

Granular, physical, and crystallographic characteristics of the sediment

Based on SEM–EDX and XRD, sediments are mainly composed of silicates, carbonates, silico-aluminates, and small quantities of Fe, K, Mg, Na, Cl, Ti, S, and P, corresponding to the following minerals: quartz, calcite, clinochlore, albite, and muscovite.

Physical and surface characteristics of sediments, such as density, water content, and BET (Brunauer–Emmett–Teller) surface area, are summarised in Table 1. Density values ranging between 2.60 and 2.72 are in agreement with XRD results, similar to mineralogical composition, mainly silica (2.65) and calcite (2.71) (Rumble 2018). Sediments contain between 26 and 31% of water. BET surface area of sediment from the basin and the channel are almost twice as great as sediment from sea (Table 1).

Morpho-granular characteristics of sediments and classification

SEM micrographs of bulk sediment shown in Online Resource Fig. S1 offer a general and detailed view of sediment particles from the basin (B), channel (C), and sea beach (Sb) areas of the Grau du Roi harbour. The general view revealed sediment particle size diversity, which ranged from sub-micron to a few hundred microns. SEM observations also revealed a diversity of sediment particle morphology: circular,

Table 1 Physical characteristics of sediment: BET surface area (S_{BET}), density (d), and water content (% water)

Sample	S_{BET} (m^2/g)	d(g/cm^3)	%water
Basin (B)	3.83 ± 0.01	2.71	26 ± 1
Channel (C)	3.91 ± 0.01		31 ± 0
Sea beach (SB)	2.21 ± 0.01		25 ± 3

granular, and platelet-shaped particles in all samples. Different types of agglomeration/aggregation can be noticed: colloid particles (< 1 μm) agglomerated/aggregated on the surface of supracolloids (1–100 μm) (Fig. 3B1) and agglomerates/aggregates of supracolloids (Online Resource Fig. S1 Sb1). Diatoms (Online Resource Fig. S1 B2) and framboidal pyrite (Online Resource Fig. S1 C2) were also observed in all samples.

Particle size distribution of bulk sediments was measured in artificial seawater; the obtained size distribution for sediment from the basin area is represented in Fig. 3a and in Online Resource Fig. S2 for sediment from the channel and the sea beach area. The size distribution curve can be used to determine the proportion of sand (63–2000 μm), silt (4–63 μm), and clay (< 4 μm) which allow the sediments to be classified according to the Classification de Udden-Wentworth (Udden 1914; Wentworth 1922) as shown in Fig. 3b. According to this classification, the studied sediments have different size characteristics; they mainly contain silt and sand in different proportions: silt loam for the basin, sandy loam for the channel, and loamy sand for the sea.

Wet sieving and classification of size fractions.

As this study investigated the role of sediment particle size on PAHs distribution and on settling behaviour, bulk sediments were divided in order to obtain sediment fractions of different granular properties according to NF ISO 3310-1, X11-514-1 standard. The following size fractions were obtained by wet sieving using artificial sea water: large fraction (80–1000 μm), intermediate fraction (40–80 μm), and fine fraction (< 40 μm). These size fractions were analysed by laser granulometry to ensure the effectiveness of the separation. An example of size fractions of sediment from the basin is shown in Fig. 3a and in Online Resource Fig. S2 for sediment from the channel and the sea beach area. The size fractions were also classified according to the Udden-Wentworth classification as presented in Fig. 3b. Classification of the different size fractions showed that they contain mainly silt, sand, and a small quantity of clay.

Only fine fractions appear to be significantly different: they do not contain sand and are more than 25% clay. This is also illustrated by surface area (Fig. 3b), large fractions, and intermediate fractions have approximately the same surface area (1.93 to 3.31 $m^2 g^{-1}$) as the bulk fractions (2.21 to 3.97 $m^2 g^{-1}$), whereas surface area of fine fractions (10.0 to 11.6 $m^2 g^{-1}$) are, as expected, five time greater than the bulk fraction. The fractions can be classified as sand-rich fractions (intermediate and large fractions) and clay-rich fractions (fine fractions).

Nevertheless, one can notice from Fig. 3a that sieving is not perfect and all fractions still contain some fine particles (particles of less than 40 μm).

Sediment PAH contamination analysis

Analyses of the 16 PAHs were performed on freeze-dried bulk sediment (< 1 mm) and size fractions (< 40 μm, 40–80 μm, and 80–1000 μm) of all sediments from the basin, channel,

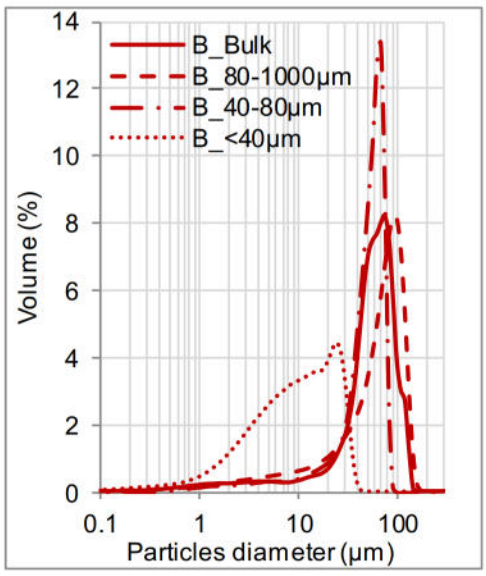

(a)

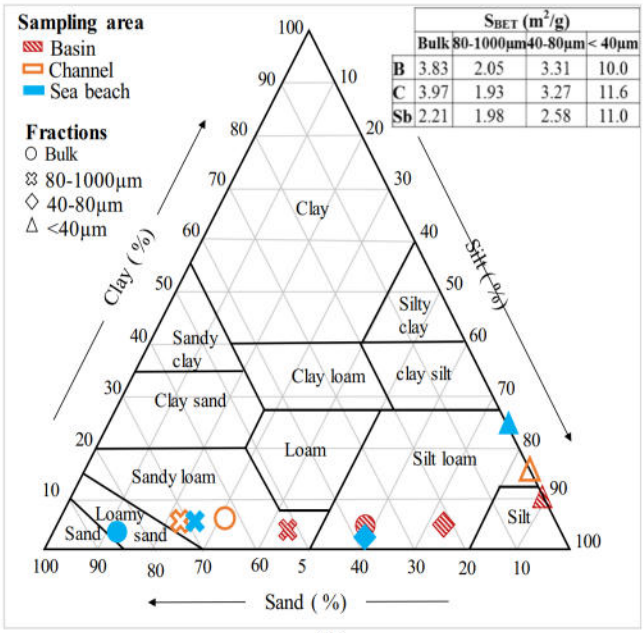

(b)

Fig. 3 Particle size distribution of bulk sediments (< 1mm) from the basin (**a**) measured in artificial seawater (A) and granular classification of the sediment in the USDA textural triangle and surface area (SBET) (**b**). Clay (< 4 μm), silt (4–63 μm), sand (63–2000 μm), and loam (mixture of sand, silt, and clay)

and sea beach. PAH contamination level and division into different size fractions, as well as parameters thought to affect PAH concentration such as particle size distribution, surface area, and organic matter content (TOC), were studied in this section. PAH distribution in size fractions will be compared and contrasted to the settling behaviour of these size fractions, in order to provide further insight into the parameters which influence PAH mobilisation during sediment resuspension events.

PAH contamination levels and repartition in different size fractions of sediment

PAH total concentrations (Σ16PAHs) of all sediments dry weight (dw) are reported in Fig. 4a. Concentrations range from 320 to 1043 μg kg^{-1}. Individual PAH composition relative to the PAH total concentration in the bulk sediments are illustrated in Fig. 4b and in Online Resource Fig. S3 for the different size fractions. Not all 16 PAHs were detected, neither naphthalene nor acenaphthylene was found in all samples. For the 14 PAHs detected in all samples, the percentage of individual PAH relative to PAH total concentration (Σ16PAHs) ranges from 1 (4 μg kg^{-1}) to 19% (180 μg kg^{-1}). The level of contamination of the sediments in the Grau du Roi harbour can be qualified as moderate (between 100 and 1000 μg kg^{-1}) according to the standard established by Baumard et al. (1998).

The bulk fraction of sediments from the basin and channel site have approximately the same level of total contamination, respectively, 491 μg kg^{-1} and 498 μg kg^{-1} while the sea beach site is the most contaminated with 857 μg kg^{-1} (Fig. 6).

Overall, individual PAH abundance in the sediment exhibited a rather moderate variability, ranging from 1 to 19%. In the size fractions (Online Resource Fig. S3), 5- and 6-ringed PAHs appeared to be the most predominate of the PAHs, making up 13 to 19% of the total composition. Three-ringed PAHs were the least abundant, composing just 1% of the sediments. The proportion of the other PAHs was around 10%. PAHs are commonly classified into two major categories: low-molecular-weight (LMW) PAHs (2 to 3 rings) and high-molecular-weight (HMW) PAHs (4 to 6 rings) (Cutroneo et al. 2015). Total proportions of HMW PAHs were higher than total proportions of LMW PAHs (9–21% for the LMW and 79–91% for the HMW) regardless of the size fraction. The predominance of HMW PAHs in sediment can be explained by the fact that they are strongly retained by sediments due to their high hydrophobicity and weak degradation (Alonso-Hernandez et al. 2014; Warren et al. 2003). It can also be justified by the origin of the PAHs found in the sediment. PAHs present in all the studied sediments were identified by the use of diagnostic ratios to be from pyrolytic origin. These ratios have been widely adopted in several studies (Abdel-Shafy and Mansour 2016; Angelico et al., 2014; Budzinski, Jones, Bellocq, Piérard, & Garrigues, 1997; Castro-Jiménez et al., 2012; Ghosh et al. 2003; Yunker et al., 2002). According to Budzinski, Jones, Bellocq, Piérard, and Garrigues (1997) and Yunker et al. (2002), PAH mixtures emitted from pyrolytic sources are enriched with PAH compounds with more than three rings. This result is in accordance with the fact that HMW PAHs are the most abundant in the studied sediments.

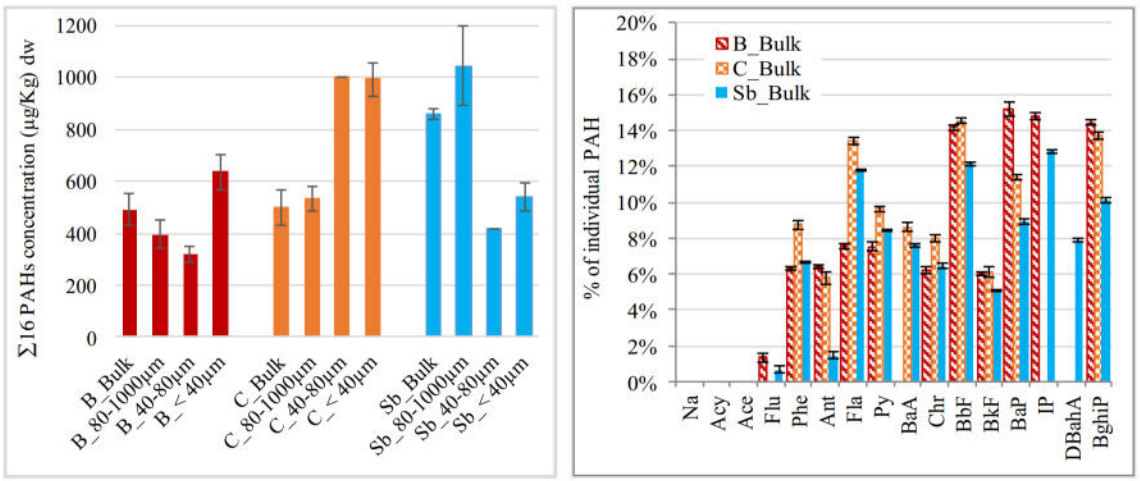

Fig. 4 PAHs total concentration (Σ16PAHs) of bulk and size fractions of sediments (**a**) and percentage of individual PAH relative to PAH total concentration (Σ16PAHs) of bulk sediments (**b**) from the basin (B), channel (C), and sea beach (Sb) areas of the Grau du Roi harbour, with naphthalene (Na), acenaphthylene (Acy), acenaphthene (Ace), fluorene (Flu), phenanthrene (Phe), anthracene (Ant), fluoranthene (Fla), pyrene (Py), benzo(a)anthracene (BaA), chrysene (Chr), benzo(b)fluoranthene (BbF), benzo(k)fluoranthene (BkF), benzo(a)pyrene (BaP), indeno (1,2,3-c,d)pyrene (IP), dibenz(ah)anthracene (DahA), benzo(ghi) perylene (BghiP)

Influence of granular characteristics and organic matter content (TOC) on PAH distribution

The possible contribution of granular characteristics such as surface area and particle size distribution as well as organic matter content to the distribution of PAHs in sediments were investigated. Total PAH concentrations were normalised to the surface area and organic matter content (TOC) of the bulk fraction and the size fractions, as illustrated respectively in Fig. 5a and Fig. 5b.

As previously shown for the bulk fraction of sediments, the sea beach site is the most contaminated with 857 μg kg^{-1} against 491 μg kg^{-1} for the basin and 498 μg kg^{-1} for channel. Even after normalising PAH concentration to surface area or organic matter content (Fig. 5a), sea beach bulk fraction still contains the most PAH by surface and by percentage of organic matter. This high contamination may be due to the location of the sediment (it was collected in the sea in front of the beach and influence from the marine currents could induced overconcentration) or to the nature of the organic matter. If the nature of organic matter of sediment from the sea beach differs from the organic matter of sediment from the basin and channel, their ability to adsorb PAHs can be different (Z. Wang et al. 2014). The contamination of this part of the harbour can represent a potential risk to the Natura 2000 site and the bathing area, which are nearby.

For size fractions of sediment from the basin and the channel sites, total PAH concentrations were higher in the intermediate and fine fractions, e.g. concentration in the large fraction is 396 μg kg^{-1} while in the fine fraction it is 635 μg.kg^{-1}. The distribution of total PAH concentration in the different size fractions of sediment from the basin and the channel are in coherence with the literature, which suggests that PAHs tend to be concentrated in fine fractions (Ahrens and Depree 2004; Maruya et al. 1996; Z. Wang et al. 2014). When normalised to organic matter content (Fig. 5b), total PAH concentrations are approximately the same, and the disparities between fine and large fractions decrease. However, when normalised to surface area (Fig. 5b), it can be noted that total PAH concentrations are higher in large fractions than in fine fractions.

In contrast, for sediment from the sea beach, the large fraction is the most contaminated with 1043 μg kg^{-1} against 539 μg kg^{-1} in the fine fraction. Even when normalised to surface area and organic matter, the PAHs repartition pattern in the size fraction stay the same. Some studies have demonstrated that PAHs can be concentrated in the coarser fractions. Ahrens and Depree (2004) found that the highest PAH concentrations were in the 125–250-μm size fraction. Similarly, X.-C. Wang et al. (2001) reported that the highest PAH concentrations were associated with the large size (> 250 μm). Both studies linked high PAH concentrations in large fractions to their high content of organic matter, but in our case, high organic matter content were found in fine fractions. Therefore, in the case of the sea beach sediment, higher PAH concentrations cannot be attributed to organic matter content. However, it may be due to the presence of finer sediment particles in the large fraction since, as previously observed in the "Wet sieving and classification of size fractions" section, after the sieving process there were still fine particles in the coarser fractions (e.g. for sediment from the sea beach site, characterisation of the large fraction indicated that particles less than 40μm represent 20% of sediment particles in the fraction).

In the size fractions, for all sediments (B, C, and Sb), PAH concentrations normalised to the surface area, show higher concentrations in large fractions than in fine fractions, meaning that large fractions adsorbed more PAHs by surface even

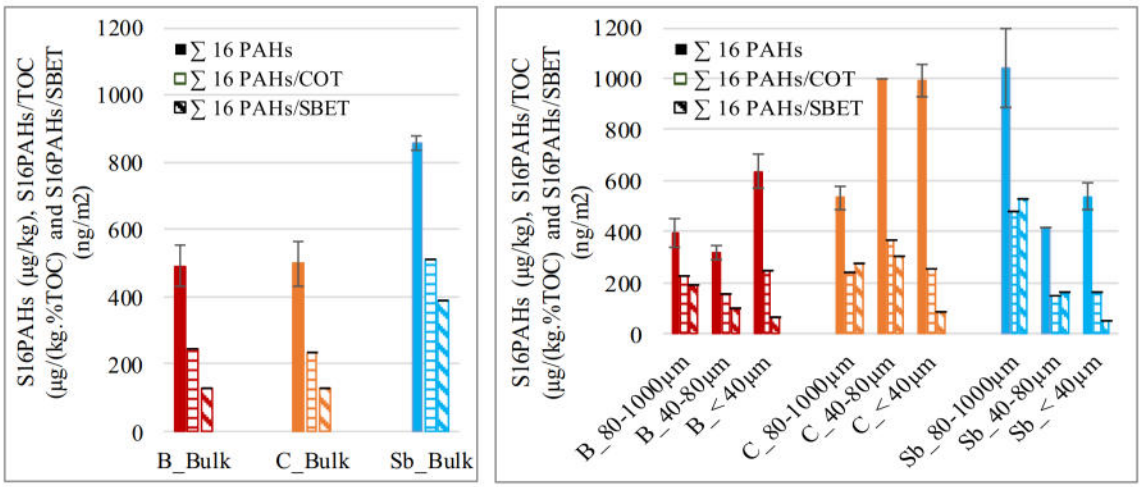

Fig. 5 Total PAHs concentration (Σ16PAHs), total PAH concentration normalised to the surface area (SBET) and organic matter content (TOC) of the bulk sediment (**a**) and of sediment size fractions (**b**) sediment from the basin (B), the channel (C), and the sea beach (Sb)

if they had lower surface area (2 to 4 $m^2\ g^{-1}$) than fine fractions (10 to 12 $m^2\ g^{-1}$). PAH concentrations normalised to organic matter were approximately the same for sediment from the basin and the channel, and for sediment from the sea beach, the disparities between fine and large fractions decrease. These results can be due to mineral surface area which affected the distribution of PAHs in sediments, as sorption of PAHs occurs either on mineral surfaces directly or in organic matter coatings on mineral surfaces (Warren et al. 2003).

Sediment settling behaviour

General evolution of sedimentation profiles

Experiments were performed with a suspension concentration of 68 g L^{-1}, corresponding to 2.5% in volume fraction Φ_V, near to the concentration (100 g L^{-1}) determined by Anger (2014) to represent dredging with hydraulic discharge.

During settling, process particles settle, following the sedimentation law proposed by Mills and Snabre (Mengual 1999), stating that the settling velocity of a particle depends on its radius and volume fraction:

$$V(\Phi, d) = \frac{V_0(d)\ (1-\Phi)}{\left[1 + \frac{K\Phi}{(1-\Phi)^3}\right]} \quad (2)$$

With: $V_0(d) = \frac{\delta\rho\ g\ d^2}{18\eta}$ and K =4.6

where $\boldsymbol{V}$ is the sedimentation velocity, Φ volume fraction, $\boldsymbol{d}$ the particle diameter, $\boldsymbol{\delta\rho}$ the density difference between the solid and liquid phases, $\boldsymbol{g}$ the gravity acceleration, and $\boldsymbol{\eta}$ the liquid dynamic viscosity.

Two zones in the sedimentation column can be noted: the "deposit" and the "supernatant" as shown in Fig. 6a, which can be clear, turbid, or fully opaque. The "deposit" formed during sedimentation is usually called "sediment", but in order to avoid confusion with sediment samples taken in the harbour, it will be called "deposit" in this study. According to their turbidity, the supernatant and the deposit can be studied either by their transmission or with backscattered profiles.

Two general kinds of sedimentation regimes can happen during the settling process: the clarification and the mass regime as shown in Fig. 7. According to Fitch (1979), at low concentrations, sedimentation by clarification regime Fig. 7a occurs, slower settling particles string out behind faster settling ones. The upper layers clarify; settled solids collect at the bottom in a deposit whose upper boundary rises as solids settle into it. On the other hand, at high concentration, particles can be held in a structure and constrained to settle at the same rate; the suspension enters a mass sedimentation regime Fig. 7b and exhibits a line-settling behaviour with a sharp interface (the sedimentation front, Fig. 7b) between the deposit and the supernatant (Fitch 1979).

Phenomena that characterise settling, such as the evolution of the supernatant and the deposit formation, were followed using two parameters. The average light transmission (T), calculated from the clarification zone shown Fig. 7 was used for the supernatant, and deposit relative height (Δh) represented Fig. 6b was used for the deposit.

In this study, sediment particles settled either by the clarification regime or by a combination of the two sedimentation regimes as is shown in Fig. 7. In some cases, after the deposit formation ,a height loss can be observed (Fig. 7a), which represents the compaction of the deposit. Mass sedimentation is distinguished from clarification, because the deposit moves downward from the top (Fig. 7b), rather than building upward from the bottom (Fig. 7a) as in sedimentation by the clarification regime.

Influence of sediment particle size distribution on settling behaviour

Sediment samples with different particle size distributions were used to investigate the influence of particle size on settling behaviour. For this purpose, settling behaviour of the bulk fractions, the large size fractions, and the fine size fractions of sediments from the basin, channel, and sea beach were

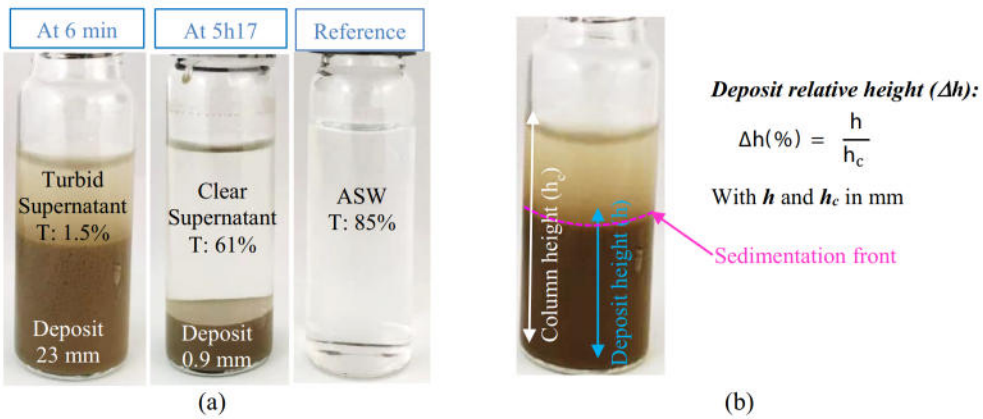

Fig. 6 Photographs of the evolution of the average transmission and the deposit height over time during settling experiments for the fine fraction (< 40μm) of sediment from the sea beach at 6 minutes, at 5.3 h and ASW (**a**) and representation of relative height (Δh) (**b**)

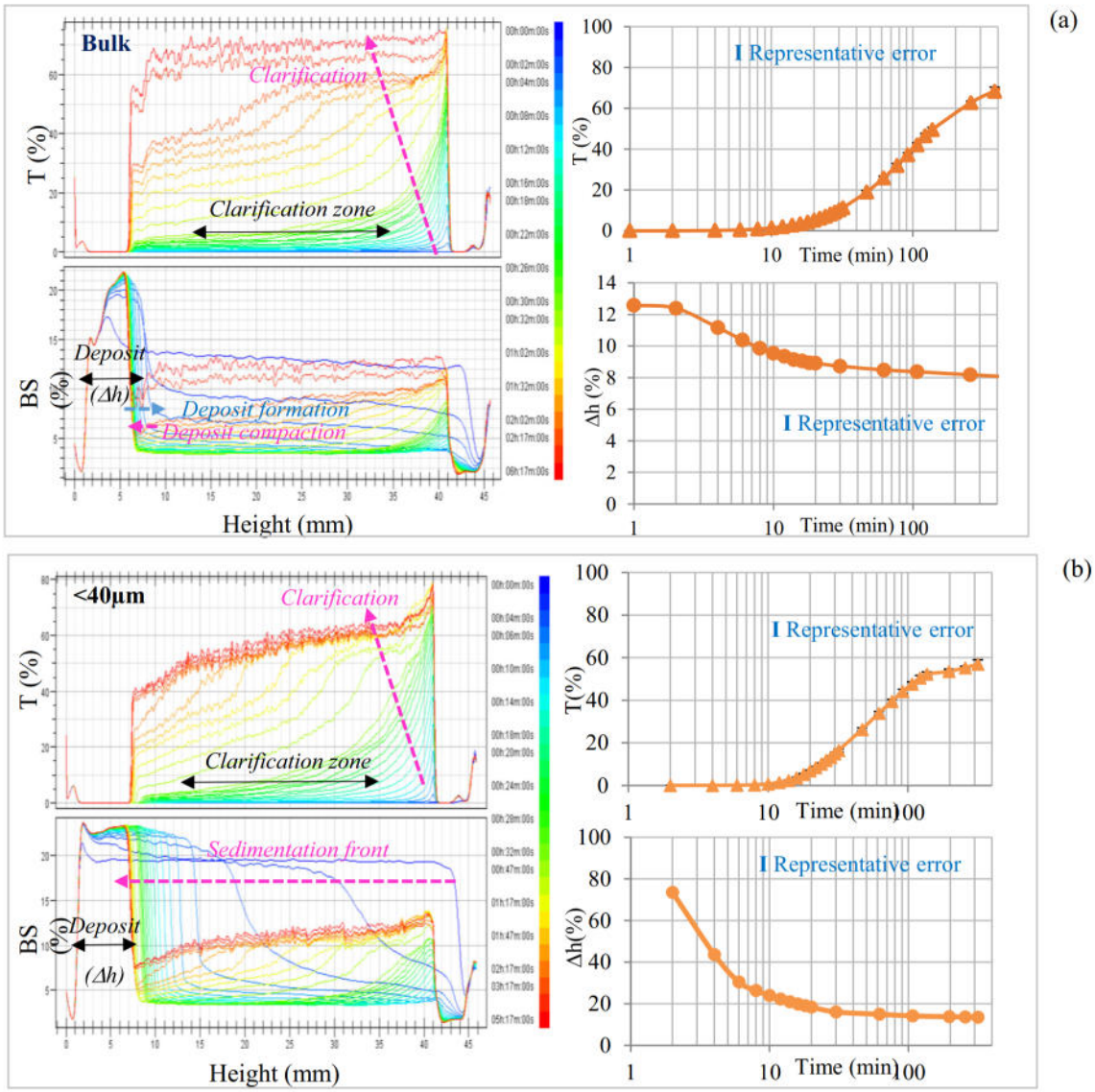

Fig. 7 Transmission profiles and the evolution of average transmission (T) over time and backscattering profiles and the deposit relative height evolution over time, during sedimentation process for the bulk fraction (**a**), and the fine fraction (**b**) of sediment from the channel

studied. Intermediate fractions were not used as they were in the same granular class as large fractions (according to the classification in section 3.3), and there was not a large enough quantity of them.

Figure 8 illustrates different types of settling behaviour exhibited by all the studied samples. All the studied sediment suspensions have the same overall evolution of the supernatant governed by sedimentation by clarification. Nothing happened in the first two minutes of the sedimentation process; then, there was an increase of transmission signal between 2 min and 4 h due to the clarification process; and finally after 4 h, the transmission signal reached a plateau (Fig. 8a).

For the bulk fraction (Fig. 8b), a deposit was formed over time, where the relative height reached its maximum (12%) in 2 min and then decreased to a plateau (8%). This shows settling by clarification of the supernatant and compaction of the deposit. The compaction may be due to the expulsion of pore water from the deposit and/or to the space filled by fine particles which settle last (Cuthbertson, Ibikunle, Mccarter, & Starrs, 2016).

In addition to the clarification regime, fine fractions also settle by mass sedimentation. This may be due to the presence of a high content of clay particles (25 to 47% of clay in the fine fractions). The mass sedimentation regime was found to be more pronounced for the sea beach fine fraction that contained the most clay (47%). This can be explained by the fact that clay particles have cohesive properties (Cuthbertson et al. 2016; Fitch 1979) that can increase the formation of a structure of sediment particles that are forced to settle together.

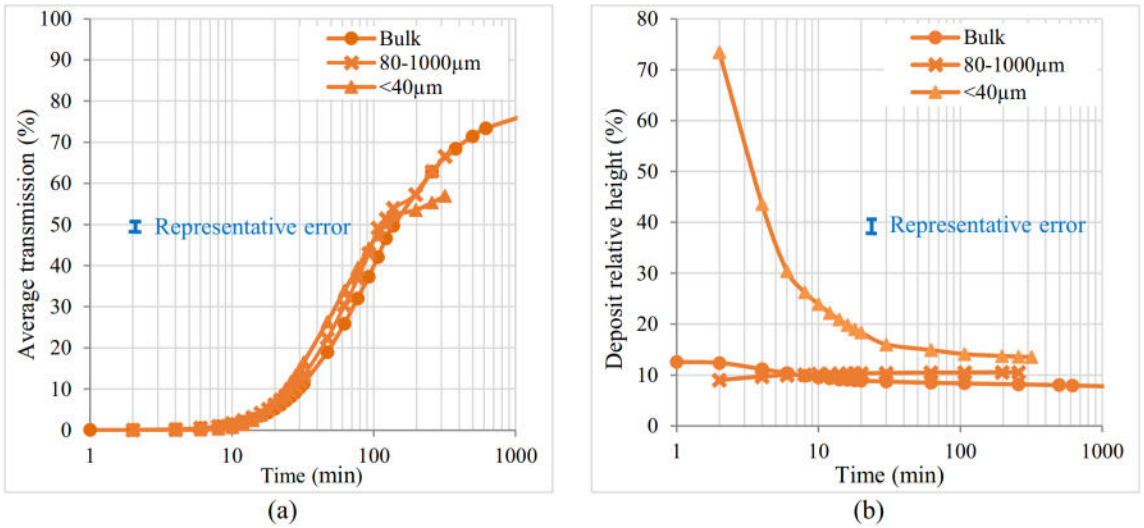

Fig. 8 Photograph of the suspension of the bulk fraction at the end of the sedimentation experiment and highlight of the two-layer deposit formed for the sediment sample from the channel

At the end of the settling process, all the samples exhibited a one-layer deposit except for bulk fractions, which ended up with a two-layer deposit, as shown in Online Resource Fig. S4. The bottom layer constituted mainly of large particles that settle first and the top layer of fine particles that settle last. The formed deposit for all the samples resulted in a particle size segregated deposit, which is in coherence with the result obtained by Cuthbertson et al. (2016).

Each studied size fraction appeared to have a different type of settling behaviour. This shows that the settling process depends on the initial particle size distribution of the sediment sample.

Laser granulometry analyses of the supernatant, performed 6 min after the initiation of settling, showed that for all samples, only particles less than 20 µm remained in the supernatant, as shown in Fig. 9a. Their granulometric evolution over time (at 0, 2, 4, 6, and 20 min) are reported in Fig. 9b for sediments from the channel area. After 4 min of settling, particles larger than 20 µm had already settled. After 20 min, particles with a maximum diameter of 15 µm still remained in suspension (with a 4- to 5 -µm mode).

The study of settling behaviour highlighted the influence of sediment particle size distribution; three different types of settling behaviour were identified depending on the sediment particle size:

Sand-rich fractions (all the large fractions and the sea beach bulk fraction) settled by clarification
Loam-rich fractions (basin and channel bulk fractions) settled by clarification and compaction
Clay-rich fractions (all fine fractions) settled by clarification and mass sedimentation

However, whatever the sedimentation mode, fine sediment particles less than 20 µm remained in the water column and could be potential vectors of pollution. These represent the greatest risk, as they constitute the fine size fraction, which was revealed to be polluted by PAHs, and shown to be the most polluted fraction from the basin and channel. In case of a resuspension event, these sediment particles (< 20 µm) seem to be the ones that can potentially displace PAHs. These results are in accordance with other studies in which fine particles were identified as potential vector of pollution in case of resuspension event : < 25 µm (Feng et al. 2008), < 60 µm (Ferré et al. 2005) and < 63 µm (Cantwell, Burgess, & King, 2008).

In addition, the fact that they can stay in suspension up to 20 min after resuspension increases the possibility for PAHs to be released by desorption into the water column. Indeed, according to a study by Dong et al. (2016) during sediment resuspension-deposition events, PAHs associated with organic carbon (OC) in suspended sediment can desorb with the release of OC and became dissolved organic carbon (DOC)–associated PAHs in the overlying water, then the PAHs can desorb from the DOC (dissolved organic carbon) and became freely dissolved.

Settling behaviour after sediment resuspension event

After sedimentation, the sample was resuspended using a paddle and the resulted settling process (resedimentation) was also studied. The induced resuspension experiment was carried out in order to mimic at a laboratory scale what occurs when sediments are resuspended in the water column during a disruption event. The resulting supernatant transmission evolution and deposit formation for all the size fractions of sediment from the channel site are reported in Online Resource

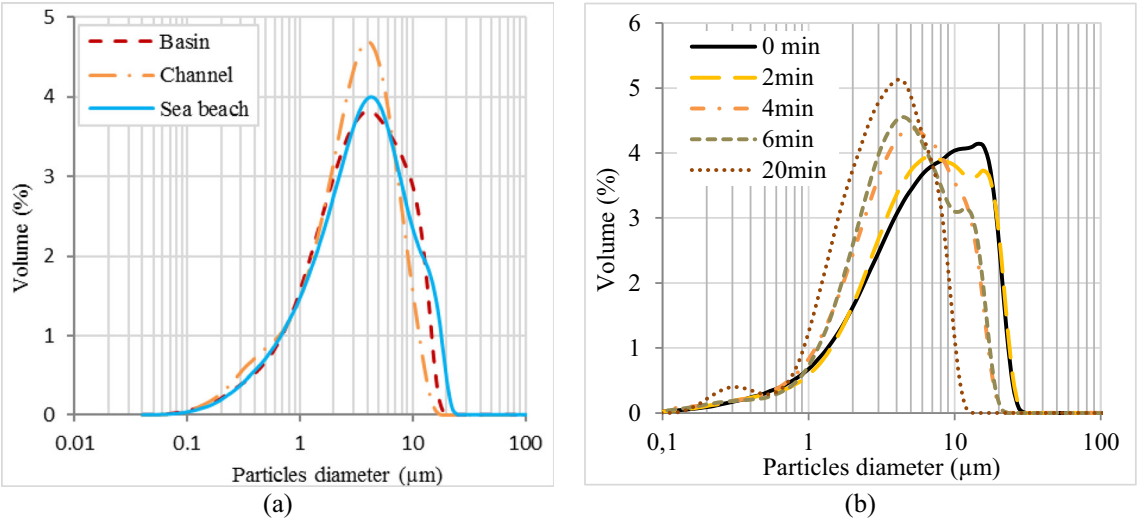

(a) (b)

Fig. 9 Particle size distribution of the supernatant of the bulk fractions at 6 min into the settling process of sediment from the basin, channel, and sea beach sites (**a**) and particles size distribution of the supernatant of the fine fraction (< 40 µm) evolution over time of the settling process for sediment samples from the channel (**b**)

Fig. S5. No significant difference was observed between the average transmission and deposit formation evolution over time for the sedimentation and the resedimentation process. This experiment allows the application of the conclusion and findings of the investigation of the sedimentation to the settling behaviour of induced resuspension on sediments (resedimentation).

Influence of volume fraction on the settling behaviour

Two sediment suspension concentrations of the two major types of dredging were chosen, in order to compare their settling behaviour. The low concentration (100 g L^{-1}) represents dredging with hydraulic discharge, while the high concentration (250 g L^{-1}) corresponds to mechanical dredging conditions (Anger 2014). In this study, the low concentration is 68 g L^{-1} (Øv = 2.5%), and the high concentration is 250 g L^{-1} (Øv = 8.5%). Suspension at low concentration will be referred to as the "diluted" suspension and suspension at high concentration as "concentrated" suspension. The experiment was performed with the fine fraction of sediment from the basin.

For these two volume fractions, particle settlement occurs both by clarification and mass sedimentation. The supernatant average transmission evolution and the deposit evolution are represented in Fig. 10. Very few differences were noted in the supernatant clarification (T = 65% against 60%), and as expected, the final deposit is larger in concentrated conditions (Δh = 35% against 14%) and the settling process takes longer (4.2 h compared to 20 min). Monitoring of sediment particle distribution during the settling process also shows that particles < 20 µm remain in the supernatant up to 20 min in the concentrated suspension as was the case in the diluted suspension previously discussed in the "Influence of sediment particle size distribution on settling behaviour" section.

Increasing the volume fraction increases only the time necessary for particles to settle and the final deposit height, but in the case of a resuspension event, the same risk for the mobilisation of PAHs by fine sediment particles (< 20 µm in this case) exists.

Conclusion

Sediments were collected in different areas (basin, channel, sea beach) of the Grau du Roi harbour, then separated into different size fractions: large (80–1000 µm), intermediate (40–80 µm), and fine (< 40 µm). Size characterisation showed that the sediment was composed of mainly silt (23–75%), small quantities of clay (3–47%), and varying quantities of sand (0–74%). Fine fractions appear to be significantly different, containing no sand, and 25 to 47% clay.

The concentrations and distributions of 16 PAHs classified US EPA priority pollutants were analysed in the bulk sediment and the three size fractions for the three samplings. Total PAH concentrations (Σ16PAHs) ranged from 320 to 1043 µg kg^{-1} and varied largely among the different size fractions. PAH distribution in the bulk sediment and the size fractions exhibited similar patterns dominated by HMW PAHs.

PAH concentrations normalised to the surface area showed higher PAHs concentrations in large fractions than in fine fractions, meaning that large fractions adsorbed more PAHs by the surface, even if they had lower surface area (2 to 4 m^2 g^{-1}) than fine fractions (10 to 12 m^2 g^{-1}). Normalisation of the PAH concentrations relative to the organic matter content made it possible to realise that the pollution was evenly

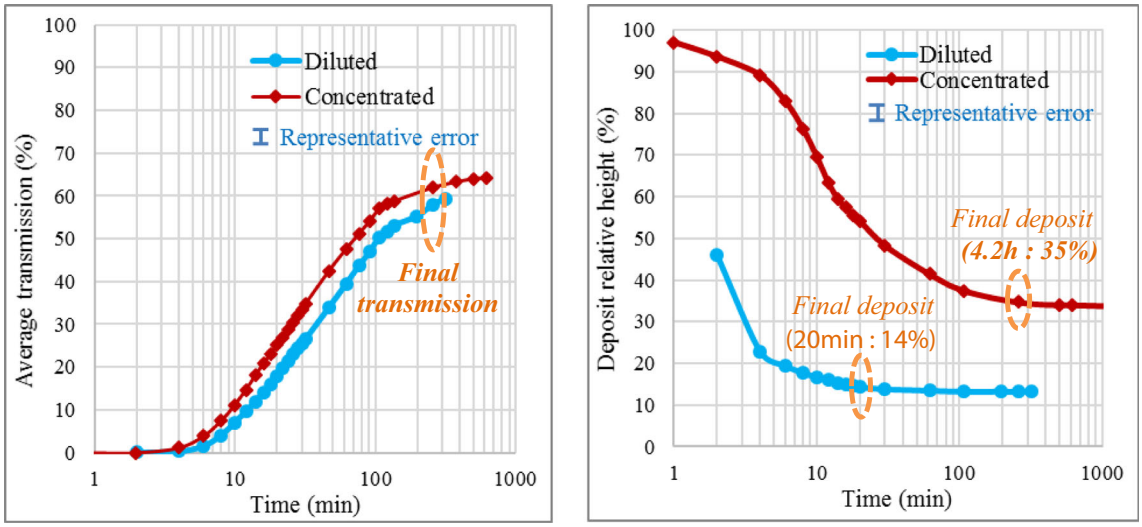

Fig. 10 Evolution of the average transmission of the supernatant (**a**), and evolution of the deposit (**b**) over time for the diluted (Øv = 2.5%) and concentrated (Øv = 8.5%) suspensions of the fine fraction of sediment from the basin site

distributed in relation to the quantity of organic matter for the bulk sediment and size fractions. PAHs concentrations varied between 160 and 370 μg kg^{-1} for 1% TOC for basin and channel sediments. On the other hand, for sea beach sediments, the concentration of PAHs in relation to organic matter in the bulk sediment and the large fraction is twice as high as in the intermediate and fine fractions.

Settling behaviour of the PAH-contaminated sediment was investigated using a non-invasive, optical analyser (Turbiscan Lab) in order to obtain better knowledge of particle sedimentation process as their presence in the water column in the case of a sediment resuspension event can result in the dispersion of PAHs into the water. Settling behaviour study revealed the influence of sediment particle size distribution. Three different types of settling behaviour were identified depending on sediment particle size distribution: clarification, clarification and compaction, and clarification and mass sedimentation. Particle size distribution monitoring during the settling allowed targeting fine sediment particles less than 20 μm, if initially present in the suspension, as the most likely to remain in the water column after resuspension, up to 20 min after the initiation of resuspension.

The sediments particles less than 20 μm in size were revealed to represent the greatest risk. Regardless of settling regime (clarification, mass sedimentation) and volume fraction (diluted, concentrated), they remained in the supernatant up to 20 min after resuspension. They are part of the fine fraction (< 40 μm), which was revealed to be polluted with PAHs, and to be the most polluted fraction of sediment from the basin and the channel. In the case of a resuspension event, these sediment particles (< 20 μm) seem to be the ones that can potentially mobilise PAHs. Furthermore, the fact that they can stay in suspension up to 20 min after resuspension increases the possibility for PAHs to be released into the water column.

Supplementary Information The online version contains supplementary material available at https://doi.org/10.1007/s11356-021-15236-z.

Acknowledgements The Région Occitanie and IMT Mines Alès are acknowledged here for supporting the present research.

Authors' contributions Gisèle Usanase (GU) performed the experimental campaign. GU interpreted and analysed the experimental results. Nathalie Azèma (NA) helped GU to perform granular and physico-chemical characterisations (settling, sediment characterisation, etc.). NA interpreted and analysed the experimental results. Youssef El Bitouri (YEB) helped GU to collect sediments and to perform granular and physico-chemical characterisations (settling, sediment characterisation, etc.). YEB interpreted and analysed the experimental results. Jean-Claude Souche (JCS) helped GU to collect sediments and to perform granular and physico-chemical characterisations (settling, sediment characterisation, etc.). JCS interpreted and analysed the experimental results. Catherine Gonzalez (CG) helped GU to perform granular and physico-chemical characterisations (sediment characterisation, PAHs characterisation). CG interpreted and analysed the experimental results.

All the authors read and approved the final manuscript.

Data availability The datasets used and/or analysed during the current study are available from the corresponding author on reasonable request.

All data generated or analysed during this study are included in this published article

References

Abdel-Shafy HI, Mansour MSM (2016) A review on polycyclic aromatic hydrocarbons: source, environmental impact, effect on human health and remediation. Egypt J Pet 25:107–123

Ahrens MJ, Depree CV (2004) Inhomogeneous distribution of polycyclic aromatic hydrocarbons in different size and density fractions of contaminated sediment from Auckland Harbour, New Zealand: an opportunity for mitigation. Mar Pollut Bull 48(3–4):341–350

Alonso-Hernandez CM, Mesa-Albernas M, Tolosa I (2014) Organochlorine pesticides (OCPs) and polychlorinated biphenyls (PCBs) in sediments from the Gulf of Batabanó, Cuba. Chemosphere 94:36–41

Anger B (2014) Caractérisation des sédiments fins des retenues hydroélectriques en vue d'une orientation vers des filières de valorisation matière. Université de Caen Basse-Normandie. https://hal.archives-ouvertes.fr/tel-01938082/

Bancon-Montigny C, Gonzalez C, Delpoux S, Avenzac M, Spinelli S, Mhadhbi T, Mejri K, Hlaili AS, Pringault O (2019) Seasonal changes of chemical contamination in coastal waters during sediment resuspension. Chemosphere 235:651–661

Barhoumi B, Lemenach K, Devier MH, Ameur WB, Etcheber H, Budzinski H et al (2014) Polycyclic aromatic hydrocarbons (PAHs) in surface sediments from the Bizerte Lagoon, Tunisia: levels, sources, and toxicological significance. Environ Monit Assess 186(5):2653–2669

Baumard P, Budzinski H, Garrigues P (1998) Polycyclic aromatic hydrocarbons in sediments and mussels of the western Mediterranean sea. Environ Toxicol Chem 17(5):765–776

Belles A, Alary C, Criquet J, Ivanovsky A, Billon G (2017) Assessing the transport of PAH in the surficial sediment layer by passive sampler approach. Sci Total Environ 579:72–81

Bourrin F, Friend PL, Amos CL, Manca E, Ulses C, Palanques A, Durrieu de Madron X, Thompson CEL (2008) Sediment dispersal from a typical Mediterranean flood: The Têt River, Gulf of Lions. Cont Shelf Res 28(15):1895–1910

Bru P, Brunel L, Buron H, Cayré I, Ducarre X, Fraux A, … Snabre P (2004) Particle size and rapid stability analyses of concentrated dispersions: use of multiple light scattering technique 45–60. https://doi.org/10.1021/bk-2004-0881.ch003

Brzozowska R, Sui Z, Kang KH (2012) Testing the usability of sea mussel (Mytilus sp.) for the improvement of seawater quality—An experimental study. Ecological Engineering 39:133–137. https://doi.org/10.1016/j.ecoleng.2011.10.017

Cantwell MG, Burgess RM (2004) Variability of parameters measured during the resuspension of sediments with a particle entrainment simulator. Chemosphere 56(1):51–58

Capello M, Cutroneo L, Consani S, Dinelli E, Vagge G, Carbone C (2016) Marine sediment contamination and dynamics at the mouth of a contaminated torrent: the case of the Gromolo Torrent (Sestri Levante, north-western Italy). Mar Pollut Bull 109(1):128–141

Chhabra RP (2019) Sedimentation. In: Chhabra RP, Gurappa B (eds) Coulson and Richardson's Chemical Engineering, 6th edn. Butterwort, pp 387–447

Coulon F (2014) Contribution à l'étude des sédiments marins lors d'opérations de dragage portuaire : re-sédimentation et mobilisation de la pollution organique. Université Montpellier II - Sciences et Techniques du Languedoc & IMT - Mines Alès. https://ged.biu-montpellier.fr/florabium/jsp/nnt.jsp?nnt=2014MON20056

Cuthbertson AJS, Ibikunle O, Mccarter WJ, Starrs G (2016) Monitoring and characterisation of sand-mud sedimentation processes. Ocean Dyn 66:867–891

Cutroneo L, Castellano M, Carbone C, Consani S, Gaino F, Tucci S, Magrì S, Povero P, Bertolotto RM, Canepa G, Capello M (2015) Evaluation of the boundary condition influence on PAH concentrations in the water column during the sediment dredging of a port. Mar Pollut Bull 101(2):583–593

Dong J, Xia X, Wang M, Xie H, Wen J, Bao Y (2016) Effect of recurrent sediment resuspension-deposition events on bioavailability of polycyclic aromatic hydrocarbons in aquatic environments. J Hydrol 540:934–946

Feng J, Shen Z, Niu J, Yang Z (2008) The role of sediment resuspension duration in release of PAHs. Sci Bull 53(18):2777–2782

Ferré B, Guizien K, Durrieu De Madron X, Palanques A, Guillén J, Grémare A (2005) Fine-grained sediment dynamics during a strong storm event in the inner-shelf of the Gulf of Lion (NW Mediterranean). Cont Shelf Res 25(19–20):2410–2427

Fitch B (1979) Sedimentation of flocculent suspensions: State of the art. AICHE J 25(6):913–930

Ghosh U, Zimmerman JR, Luthy RG (2003) PCB and PAH speciation among particle types in contaminated harbor sediments and effects on PAH bioavailability. Environ Sci Technol 37(10):2209–2217

Guigue C, Tedetti M, Huy Dang D, Mullot J-U, Garnier C, Goutx M (2018) Remobilization of polycyclic aromatic hydrocarbons and organic matter in seawater during sediment resuspension experiments from a polluted coastal environment: Insights from Toulon Bay (France). https://hal.archives-ouvertes.fr/hal-01635969

Hayes DF (1986) Development of a near field source strength model to predict sediment resuspension from cutter suction dredges. Mississippi State University. https://mlp.ent.sirsi.net/client/en_US/msstate/search/detailnonmodal/ent:002fSD_ILS002fSD_ILS:169822/ada?rt=CKEY|||CKEY|||false

Huntingford EJ, Turner A (2011) Trace metals in harbour and slipway sediments from the island of Malta, central Mediterranean. Mar Pollut Bull 62(7):1557–1561

IARC (1983) Polynuclear aromatic compounds, part 1, chemical, environmental, and experimental data. 32:1-453. PMID: 6586639. https://monographs.iarc.fr/wpcontent/uploads/2018/06/mono32.pdf

Je C h, Hayes DF, Kim K-s (2007) Simulation of resuspended sediments resulting from dredging operations by a numerical flocculent transport model. Chemosphere 70(2):187–195

Latimer JS, Davis WR, Keith DJ (1999) Mobilization of PAHs and PCBs from in-place contaminated marine sediments during simulated resuspension events. Estuar Coast Shelf Sci 49(4):577–595

Maruya KA, Risebrough RW, Horne AJ (1996) Partitioning of polynuclear aromatic hydrocarbons between sediments from San Francisco Bay and their porewaters. Environ Sci Technol 30(10):2942–2947

Mengual O (1999) TURBISCAN MA 2000: multiple light scattering measurement for concentrated emulsion and suspension instability analysis. Talanta 50(2):445–456

NF ISO 3310-1, X11-514-1 (07/2019) Metal wire cloth and perforated plate for test sieves-technical requirements and verifications. https://www.normadoc.com/french/nf-x11-514pr-pr-nf-iso-3310-1-02-2019.html

Rumble JR (2018) CRC Handbook of Chemistry and Physics. CRC Press, Ed., 99th ed. Boca Raton, Taylor & Francis

Simpson CD, Mosi AA, Cullen WR, Reimer KJ (1996) Composition and distribution of polycyclic aromatic hydrocarbon contamination in surficial marine sediments from Kitimat Harbor, Canada. Sci Total Environ 181(3):265–278

Spearman J (2015) A review of the physical impacts of sediment dispersion from aggregate dredging. Mar Pollut Bull 94(1–2):260–277

Udden JA (1914) Mechanical composition of clastic sediments. Geol Soc Am Bull 25:655–744. https://doi.org/10.1130/gsab-25-655

United States Environmental Protection Agency (USEPA) (1993) Provisional Guidance for Quantitative Risk Assessment of Polycyclic Aromatic. U.S. Environmental Protection Agency, Office of Research and Development, Office of Health and Environmental Assessment, Washington, DC, EPA/600/R-93/089 (NTIS PB94116571).

Vagge G, Cutroneo L, Castellano M, Canepa G, Bertolotto RM, Capello M (2018) The effects of dredging and environmental conditions on concentrations of polycyclic aromatic hydrocarbons in the water column. Mar Pollut Bull 135:704–713

Wang X-C, Zhang Y-X, Chen RF (2001) Distribution and partitioning of polycyclic aromatic hydrocarbons (PAHs) in different size fractions in sediments from Boston Harbor, United States. Mar Pollut Bull 42 (11):1139–1149

Wang Z, Liu Z, Xu K, Mayer LM, Zhang Z, Kolker AS, Wu W (2014) Concentrations and sources of polycyclic aromatic hydrocarbons in surface coastal sediments of the northern Gulf of Mexico. Geochem Trans 15(1):2

Warren N, Allan IJ, Carter JE, House WA, Parker A (2003) Pesticides and other micro-organic contaminants in freshwater sedimentary environments - a review. Applied Geochemistry 18(2):159–194

Wendling V, Gratiot N, Legout C, Droppo IG, Coulaud C, Mercier B (2015) Using an optical settling column to assess suspension characteristics within the free, flocculation, and hindered settling regimes. J Soils Sediments 15(9):1991–2003

Wentworth CK (1922) A Scale of Grade and Class Terms for Clastic Sediments. J Geol 30:377–392. https://doi.org/10.1086/622910